

Influence of the Molecular Surface Characteristics of the Diastereoisomers of a Quartet Molecule on their Physicochemical Properties: A Linear Solvation Free-Energy Study

Nora Ventosa,^[a] Daniel Ruiz-Molina,^[a] Josep Sedó,^[a] Concepció Rovira,^[a] Xavier Tomas,^[b] Jean-Jacques André,^[c] André Bieber,^[c] and Jaume Veciana*^[a]

Abstract: The influence of the molecular surface characteristics on the ability of a molecule, the quartet 2,4,6-trichloro- $\alpha,\alpha,\alpha',\alpha',\alpha'',\alpha''$ -hexakis(penta-chlorophenyl)mesitylene (**1**), to interact with the neighboring solvent molecules is studied. As physicochemical properties for this study we chose the influence of the surrounding medium on the differential chromatographic retention of two atropisomeric forms of **1**, the diastereomers with C_2 and D_3 symmetries, the isomerization equilibrium between these two diastereomers, and their tumbling processes in solid or viscous amorphous matrices, as observed by ESR spectroscopy. In these studies we have employed *linear solvation free*

energy relationships (LSER), considering as the most important solute/solvent interactions the cavitation effect, the dipolarity/polarizability, and the hydrogen-bonding ability of the solvent. In order to use such an LSER approach efficiently, a general classification of classical organic solvents in eleven different categories has been carried out. The results of this study demonstrate that the shape and roughness (fractality) of the diastereomers of quartet **1** are

Keywords: high-spin molecules • isomerizations • linear free-energy relationships • solvent effects • surface analysis

among their most important molecular characteristics in relation to their ability to interact with the surrounding media. These molecular parameters modify the studied properties mainly as a result of cavitation effects. In contrast, when the cavitation effects are not important, as occurs with the tumbling of the isomers inside the preformed cavities of the solvent, the unique molecular parameter that discriminates the behavior of both stereoisomers seems to be the dipolarity/polarizability. From this study we can conclude that the intrinsic surface characteristics of this molecule plays an influential role in many of its physicochemical properties.

Introduction

The study of the influence of solvents on the physical or chemical properties of a solute is an area of the utmost importance, since most chemical processes take place in solution. There is an increasing trend on the chemical community to endeavor to interpret the thermodynamic


behavior of chemical systems in fluid media in terms of molecular parameters and intermolecular interactions. Among the molecular parameters related with the thermochemical activity of a solute are the chemical groups or functions responsible for the specific interactions with the solvent molecules, and others which account for nonspecific interactions, such as the size, shape, and surface area.^[1–4] While the influence of the first kind of molecular parameters on the physicochemical properties is relatively well understood, the exact role of the second type of parameters has yet to be established. Therefore, there is a need to address, both experimentally and theoretically, a variety of systems involving different types of intermolecular forces in order to study how the size, shape, and surface area influence the physicochemical properties of a solute.

Langmuir, in 1925, was the first to introduce the concept of superficial area of a solute to determine its thermochemical activity.^[1] He considered that the energy required to build a cavity in the solvent was an important factor in relation to solubility and was therefore proportional to the solute area.

[a] Prof. J. Veciana, Dr. C. Rovira, Dr. N. Ventosa, Dr. D. Ruiz-Molina, Dr. J. Sedó
Institut de Ciència de Materials de Barcelona (CSIC)
Campus de la Universitat de Bellaterra, E-08193 Cerdanyola, (Spain)
Fax: (+34) 93-5805729
E-mail: vecianaj@icmab.es

[b] Prof. X. Tomas
Institut Químic de Sarrià (Universitat Ramon LLull)
Via Augusta 390, E-08017 Barcelona (Spain)

[c] Prof. A. Bieber, Prof. J.-J. André
Institut Charles Sadron (CNRS)
6 rue Boussingault, F-67083 Strasbourg (France)

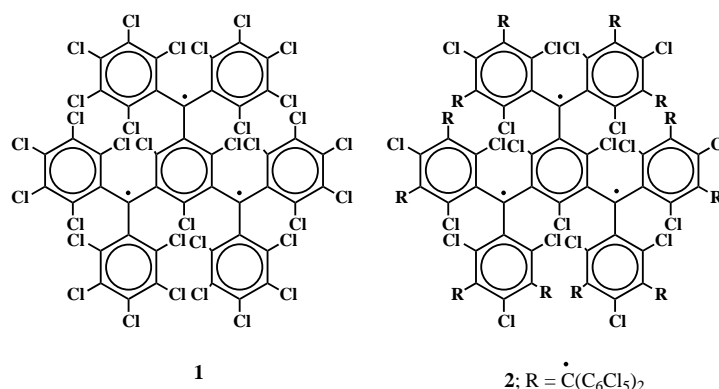
 Supporting information for this article is available on the WWW under <http://www.wiley-vch.de/home/chemistry/> or from the author.

Subsequently, many studies have been developed based on models and methods that explain and calculate the interaction of a molecule with its surroundings through consideration of its surface area as well as the molecular volume.^[2] On the other hand, Pauling postulated that the interactions among macromolecules of biological interest, such as nucleic acids and proteins, are modulated first and foremost by their size and shape.^[3]

The importance of surface characteristics on the behavior of macromolecules, either biological or synthetic, has promoted the design of computational methods suitable for the calculation and study of molecular surfaces.^[4] However, as far as we know, a firm, experimental verification highlighting the influence of fractal character and surface area on the physicochemical properties of synthetic macromolecular systems has been lacking. The most likely reason for this absence is that the great majority of macromolecules have low symmetry and high flexibility and, therefore, they exist in an overwhelming number of interconverting conformations, which are difficult to characterize theoretically and detect in solution. The ideal molecular system to be used as a model for the quantification of the importance of its surface characteristics on its physicochemical properties is a single molecule with high enough symmetry and structural rigidity. These characteristics encourage the existence of a limited number

of diastereomeric conformations, with a high enough diastereoisomerization barrier to ensure that each conformation has a sufficient lifetime in solution to be studied separately.

Here we report a comprehensive study confirming the influence of the molecular surface characteristics on the ability of a molecule to interact with neighboring solvent molecules. To reach this target, we have used the molecule **1**, which has a quartet ground state and corresponds to the first generation of the high-spin dendrimer series shown in Scheme 1 (molecule **2** is the second generation).^[5-6]



Scheme 1.

Abstract in Catalan: *En aquest treball s'estudia la influència de les característiques de la superfície molecular del quartet 2,4,6-tricloro- α,α,α' , α' , α'' , α'' -hexaquis(pentacloro-fenil)mesitilè (**1**) en la seva capacitat per a interaccionar amb les molècules veïnes de dissolvent. Per a realitzar aquest estudi, s'analitza la influència del medi en la retenció diferencial cromatogràfica de les dos formes atropisomèriques del quartet **1**-els diastereoisòmers C_2 -**1** i D_3 -**1**, així com en l'equilibri d'isomerització i en el procés de volteig molecular, observat per ESR, en una matriu sòlida amorfa. L'estudi d'aquests processos físicoquímics s'ha realitzat a la llum de la relació lineal d'energia lliure de solvatació (LSER), considerant que la cohesivitat, la dipolaritat/polaritzabilitat, i la capacitat d'establir ponts d'hidrogen del medi són els paràmetres més importants que governen les interaccions entre solut i dissolvent. A fi d'emprar de manera adequada la teoria de la LSER, s'ha realitzat una classificació dels dissolvents orgànics més comuns en onze categories. La conclusió més important d'aquests estudi és que la forma i la rugositat (fractalitat) dels diastereoisòmers del quartet **1** són les característiques moleculars més importants que controlen la seva interacció diferencial amb el medi. La importància d'aquests paràmetres moleculars és nul·la quan el procés físicoquímic no implica la formació de cavitats, com succeeix en el volteig de les molècules en una matriu sòlida amorfa. En aquest cas, el paràmetre discriminador sembla ser la dipolaritat/polaritzabilitat. Per tant, d'aquest estudi es desprèn que les característiques intrínseques de la superfície molecular dels dos diastereoisòmers del quartet **1** juguen un paper molt important en el govern del comportament físicoquímic diferencial d'ambdós isòmers.*

Quartet **1** is an exceptional molecule in the sense that it exists in two isolable and stable diastereomeric forms that show differences in their overall shapes and external surfaces, as well as in their physicochemical properties. Furthermore, as occurs for most macromolecules, these stereoisomers interconvert, but remarkably this process can be quenched just by lowering the temperature; this is as a result of the high conformational rigidity of this molecule. Since the structural features of each stereoisomer of **1** are different and well defined, such isomers are ideal models for studying the influence of the molecular surface characteristics on the control of a physicochemical property or process.

The experimental results obtained with the two stereoisomers of **1** were interpreted with the linear solvation free-energy relationship (LSER) theory, which provides chemical insights into the solvent/solute and solvent/solvent molecular interactions that impact most strongly on the process under analysis.^[7] As physicochemical processes for our study, we chose the differential chromatographic retention of both isomers of **1**, the dependence of the equilibrium constant of the diastereoisomerization on the nature of the surrounding medium, and the variation of the tumbling rate of each stereoisomer inside different solid or viscous amorphous matrices.

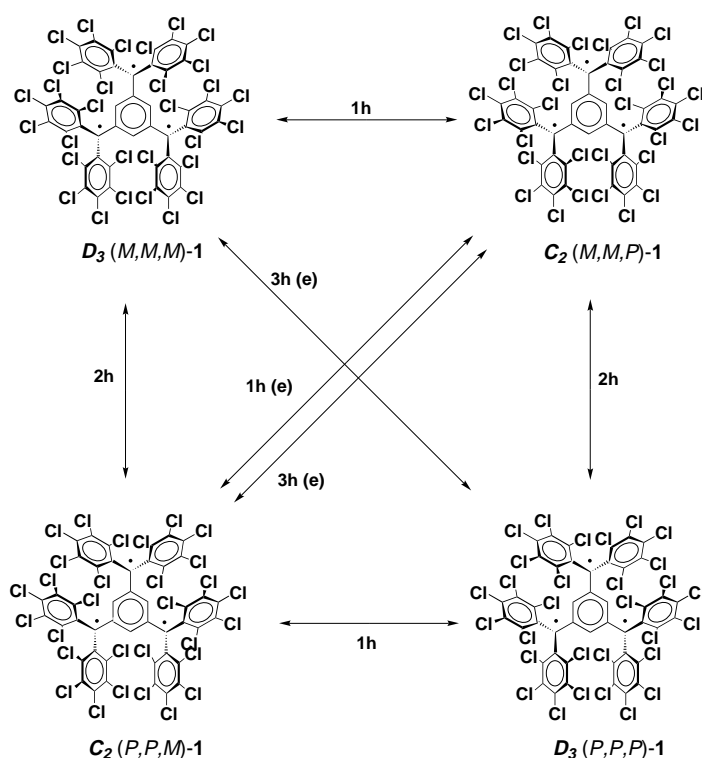
Results and Discussion

Stereochemical and structural characterization of the diastereoisomers of **1:** Before describing the study of the influence of the distinct molecular parameters of the diastereoisomers of

quartet **1** on their interactions with neighboring solvent molecules, it is necessary to give a detailed description of the structural and electronic characteristics of these stereoisomers.

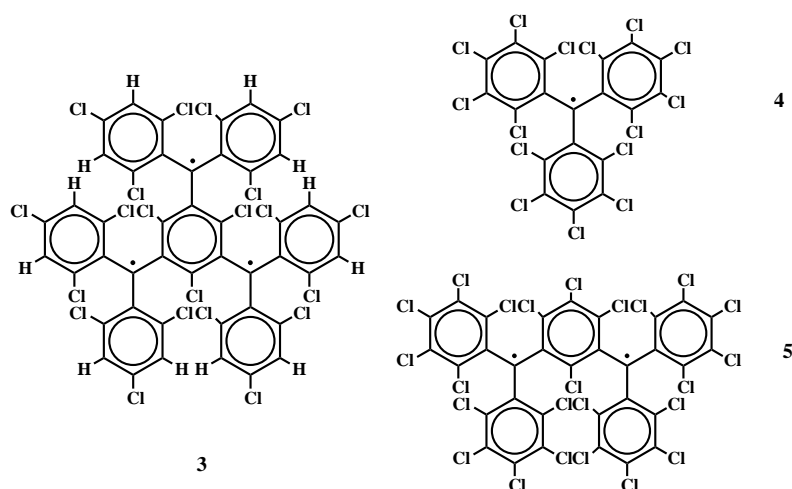
It is well known that molecules of the type Ar_3Z , in which three aryl groups (Ar) are bonded to a central Z atom, which in turn may have either an sp^2 or sp^3 hybridization, are propeller-like in shape. A large number of theoretical studies on the stereochemistry of these propeller-like systems were performed by Mislow et al.^[8] They established that in the most simple cases, where the three aryl groups (blades) are not substituted, or else symmetrically substituted around the $C_{ar}-Z$ bond axis of each aryl group (i.e., groups with local C_2 axes), the molecule has always at least two enantiomeric forms due to the intrinsic stereogenic element—*helicity*—of any propeller that provides chirality to the molecule. If the helix adopts a clockwise sense the enantiomer is called *Plus* (*P*), whereas if it adopts the opposite sense is called *Minus* (*M*). In the case that the substituents of the aryl rings no longer lie along the $C_{ar}-Z$ bond axis new kinds of stereoisomers appear. The maximum number of isomers for each substitution pattern depends on the number and nature of the isomeric degeneracy; several experimental studies exist that confirm such theoretical predictions.^[8] By contrast, very few similar studies have been reported on molecules with two or more propeller-like units. Quartet **1** is one of such rare molecules, since it has three propeller-like subunits arranged symmetrically around one common, central aromatic ring. Accordingly, for its stereochemical analysis, the molecule can be considered as an assembly of three Ar_2ZAr' subunits. Since all the six outer Ar groups of this molecule possess local C_2 axes that are coincident with their bonds to the three Z atoms, and such atoms have an sp^2 hybridization, the molecule has only three stereogenic elements. Therefore, the maximum number of stereomeric forms expected for **1** are $2^3=8$ (four D/L pairs) stereoisomers. However, since the six outer Ar groups and the three central carbon atoms are identical, there must be an isomeric degeneracy. Thus, the three D/L pairs with one of the three propeller-like subunits differing in their helicity with respect to the two others become equivalent. Consequently only the two D/L pairs with D_3 and C_2 symmetries, depicted in Scheme 2, are actually distinct.

These two diastereomeric forms show an overwhelming persistency with lifetimes of years, being resolved and isolated by HPLC chromatography or by crystallization as stable solids.^[5] The structural assignment of both stereoisomers was performed by means of the ESR spectra of frozen, diluted solutions of both forms, since this technique is particularly sensitive to the molecular symmetry. Thus, the most stable and abundant diastereomeric form, which is also the least



retained one under achiral reversed-phase liquid chromatography, was assigned to that with C_2 symmetry.^[5] Afterwards, such a structural assignment was confirmed by the resolution of the crystal structures of the two diastereomers of a structurally similar high-spin molecule: the 2,4,6-trichloro- $\alpha,\alpha,\alpha',\alpha',\alpha'',\alpha''$ -hexakis(2,4,6-trichlorophenyl) mesitylene quartet (**3**) (Scheme 3).^[9] The symmetries and, therefore, the ESR signals of diastereoisomers of **3** are expected to be identical to those of quartet **1**.

Molecular geometries and relative stability: In order to determine the molecular geometry and relative stability of the stereoisomers of quartet **1**, AM1 semiempirical calcula-



tions were done on molecular models with C_2 and D_3 symmetries. It should be noted that full geometry optimizations with configuration interactions (CI) is extremely time demanding, especially when they involve a high number of heavy atoms, as for quartet **1**. On account of the structural rigidity of the molecule, a reasonable alternative consisted in carrying out the geometry optimization with an UHF wavefunction. The optimized structures were then used as input geometries for a single-point CI calculation, which allowed a more accurate estimation both of the electronic properties and the heat of formation corresponding to each of the above-mentioned diastereomeric forms.

The most relevant structural parameters of the *in vacuo* AM1-UHF-optimized geometries of isomers C_2 and D_3 are summarized in Table 1, together with those obtained with the

Table 1. Bond lengths [pm], bond angles [°], and torsion angles [°] calculated by UHF-AM1 for radical **4** and the diastereomers of quartet **1**.

Structural parameters ^[a]	4	Mean values	
		1-C₂	1-D₃
C _{rad} ...C _{ipso(int)}	–	145.2	145.5
C _{rad} ...C _{ipso}	145.2	145.3	145.2
C _{ipso} ...C _{ortho}	141.9	141.9	142.0
C _{ortho} ...C _{meta}	140.9	140.9	140.9
C _{meta} ...C _{para}	140.9	140.9	140.9
C _{ortho} ...Cl	169.1	169.2	169.1
C _{meta} ...Cl	169.0	169.0	169.0
C _{para} ...Cl	168.8	168.8	168.8
C _{ipso(int)} ...C _{ortho(int)}	–	142.0	141.9
C _{ortho(int)} ...Cl	–	169.3	168.9
C _{ipso} ...C _{rad} ...C _{ipso}	120.0	120.0	120.0
C _{ortho} ...C _{ipso} ...C _{rad}	120.9	120.9	120.9
Cl...C _{ortho} ...C _{ipso}	120.5	120.5	120.5
Cl...C _{ortho} ...C _{meta}	118.6	118.6	118.6
C _{meta} ...C _{ortho} ...C _{ipso}	120.9	120.9	120.9
C _{ortho} ...C _{ipso} ...C _{ortho}	118.2	118.2	118.2
C _{ortho(int)} ...C _{ipso(int)} ...C _{ortho(int)}	–	118.3	120.0
C _{ipso(int)} ...C _{ortho(int)} ...C _{ipso(int)}	–	121.6	120.0
Cl...C _{ortho(int)} ...C _{ipso(int)}	–	119.1	120.0
C _{ortho} ...C _{ipso} ...C _{rad} ...C _{ipso}	± 50.4 ^[b]	– 50.0/+ 50.5 ^[b]	± 50.5 ^[b]

[a] Atomic subindex “int” means that the corresponding atom belongs to the internal aromatic ring of the quartet; “rad” = tertiary carbon with sp² hybridization. [b] The positive or negative sign of the torsion angle indicates, respectively, a *P* or *M* helicity of the propeller-like subunit.

same methodology for a simple and structurally analogous model compound, the perchlorotriphenylmethyl radical **4**. The most striking feature arising from these geometrical data is the extraordinary similarity between the values taken by the geometric parameters of radical **4** and those of quartet **1**. This is already a clear indication that the existence of two extra diarylmethyl moieties in **1**, as compared with **4**, has an almost negligible structural effect. In other words, in quartet **1** the three propeller-like moieties may be safely considered independent from each other, so that no significant geometrical distortions arise from their proximity. The estimated standard heats of formation, which proved to be only 1.7 kJ mol^{–1} lower for the C_2 diastereomer, also provides strong evidence for this independence. Therefore, in terms of energy the diastereomers of quartet **1** can be considered nearly isoenthalpic. If we take into account that entropic

factors intrinsic to the molecule depend exclusively on its molecular symmetry and can therefore be sharply defined, as shown below, we come to the conclusion that the diastereomeric forms of quartet **1** qualify as excellent candidates for the study of conformational equilibria dominated by solute/solvent interactions. AM1-CI semiempirical calculations provide additional valuable information concerning the physicochemical properties of quartet **1**. As a matter of fact, the ground state is shown to be a quartet, $S = 3/2$, (high spin) for both diastereomers, in accordance with experimental data published elsewhere.^[5] Last but not least, the energetic gap between the quartet ground state and the first excited (low spin) doublet state amounts to about 0.1 eV (10 kJ mol^{–1}) for both isomers, which would fully explain why the population of this first excited state is negligible even at room temperature, that is, why the high-spin ground state is so robust, in spite of the lack of planarity of the π -delocalized system. Finally, the calculated dipole moments obtained for both isomers are in accordance with their molecular symmetries. Thus, the zero dipole moment found for the D_3 isomer (with only one C_3 and three C_2 rotation axes) is in agreement with its ternary symmetry, whereas the value for the C_2 isomer is 0.09 Debye.

Molecular surface characteristics of diastereomers: A precise description of the overall size, shape, and outside surface characteristics of any molecule can be obtained by use of the concept of molecular surface (MS).^[4, 10] The MS defined by Richards is composed of two parts: the contact surface and the re-entrant surface.^[4c] The contact surface is the part of the van der Waals surface of each atom that is accessible to a probe sphere of a given radius r . The re-entrant surface is defined as the inward-facing part of the probe sphere when it is simultaneously in contact with more than one atom; this depends strongly on the size of the probe sphere used to determine the MS area. The resulting MS area (A_{MS}) is a continuous function of the probe radius, $A_{MS} = f(r)$, which can be calculated by different algorithms and programs and is extremely useful for studying nonspecific solute/solvent interactions.^[4d, 11, 12] Figure 1 (top) shows the distinct MSs exhibited by the D_3 isomer of quartet **1** when calculated with its UHF-AM1-optimized geometry with spherical probes of effective radii (r) of 200 and 1000 pm. Also MSs of the D_3 and C_2 isomers obtained with spherical probes of $r = 250$ pm are shown in Figure 1 (bottom) and exhibit the differences in their roughness.

Another structural feature relevant to nonspecific solute/solvent interactions is the texture or roughness of the molecular surface.^[13] The degree of irregularity or roughness is an important factor in considering such interactions and can be described by the fractal dimension (D) of the MS.^[13] As a surface becomes more irregular the fractal dimension changes from the value $D = 2$, for an ideal smooth surface, to values of $D \leq 3$. From Equation (1) the value of the magnitude of $(2 - D)$ may be obtained from the slope of the plot of $\log(A_{MS})$ against $\log(r)$ and is used to define the MS.

$$2 - D = d \log(A_{MS}) / d \log(r) \quad (1)$$

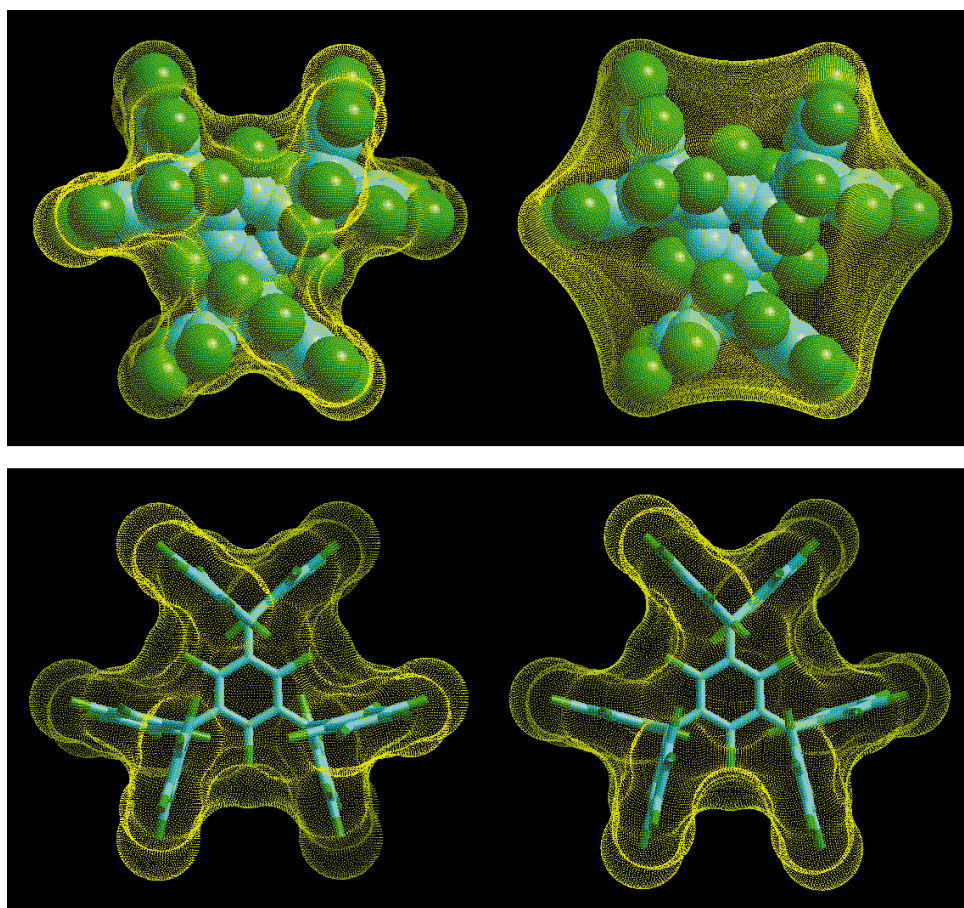


Figure 1. Calculated molecular surfaces (yellow dots): *Upper*: molecular surfaces of the D_3 isomer of quartet **1** from spherical probes with effective radii of 200 pm (left) and 1000 pm (right). *Lower*: Molecular surfaces of the C_2 (right) and D_3 (left) isomers by using a probe with an effective radius of 250 pm.

The relation between the molecular surface area and the size of the probe spheres for the D_3 and C_2 isomers, shown in Figure 2, were calculated by using their UHF-AM1 optimized geometries. Figure 2 also shows the dependence of the fractal dimension of both isomers on the probe radius obtained from Equation (1). The studied probe radii range of 200–600 pm includes the effective sizes of most of the organic solvent molecules and side chains of chromatographic stationary phases. It must be emphasized that the behaviour of the fractal dimension for the isomers of quartet **1** is very similar to that described for other macromolecules and biologically related systems.^[14] Thus, the smallest probes have access to all the solute cavities and then can form contacts with the van der Waals spheres that describe the atomic framework of the molecule (see Figure 1). In this case the fractal dimension is close to that expected for an ideal smooth surface ($D = 2$). An increase of the probe size leads to a decrease in A_{MS} , since the probe now has no accessibility to all the solute cavities, and as a consequence the fractal dimension increases as expected for a rougher surface. Finally, for very large probe sizes the fractal dimension of both isomers decreases until a stationary value of two is reached, since these probes can only see a smooth envelope contour, as shown in Figure 1 for a probe radius of 1000 pm. It is interesting to analyze the fractal dimension and the A_{MS} of both isomers for probes that have radii similar to those exhibited by most of the organic solvents,

that is, 200–600 pm. For such probe sizes, the fractality of the C_2 isomer is somewhat larger than that of the D_3 isomer owing to the large roughness of the first isomer produced by its highly cleft surface. This molecular characteristic makes the A_{MS} of C_2 smaller when compared with the other isomer. Therefore, the D_3 isomer has more chances to interact with the neighboring solvent molecules through nonspecific solute/solvent interactions, since it has a more accessible surface.^[4d, 11, 12]

Kinetic study of the diastereomerization process: Up to now we have shown that quartet **1** exists in two different diastereomers that are nearly isoenthalpic and show distinct structural characteristics such as symmetry, size, shape, and fractality. Another important feature that makes this molecule exceptional is its high energy barrier of isomerization, since it permits to freeze or promote the diastereomerization process just by changing the temperature. Stereomerizations in Ar_3Z systems can be envisioned through several different mechanisms. However, since all of these processes take place through highly hindered correlated torsional motions of the aryl groups around the $C_{ar}-Z$ bonds only few of them will be energetically accessible. Mislow et al. showed that the lowest energy mechanism—or threshold mechanism—for such a process is the “two-ring flip” mechanism, in which two aryl groups rotate simultaneously in one direction, while the third

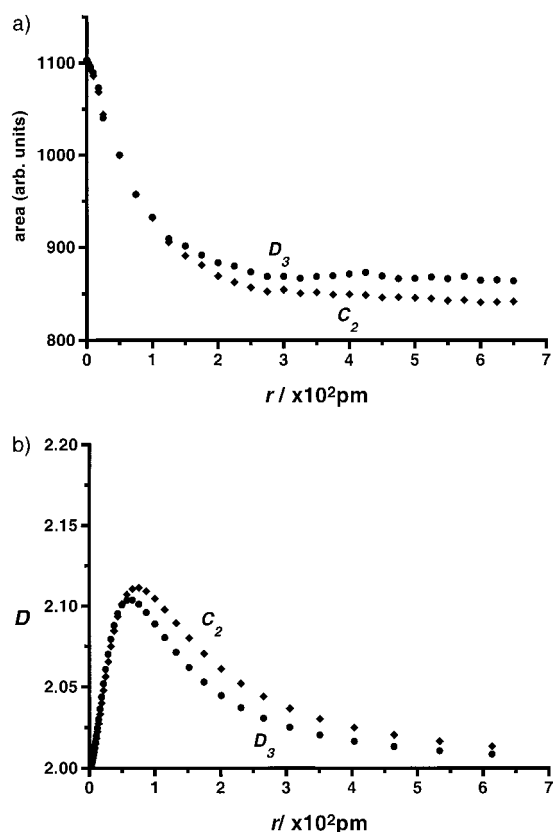


Figure 2. Dependencies of the a) area (A_{MS}) and b) fractal dimension (D) of solvent-accessible surfaces of D_3 and C_2 isomers of quartet **1** on the probe-sphere radius.

one rotates in the opposite direction.^[8] According to such considerations, the interconversion between the C_2 and D_3 diastereomers must take place through this threshold mechanism, either through an uncorrelated reversal of the helicity of one of the three Ar_2ZAr' subunits (epimerization) or by a correlated process involving two or three of such subunits. Scheme 2 summarizes the seven possible interconversion pathways between the four stereoisomers of quartet **1**. Three such pathways involve the helicity reversal of one of the propeller subunits (**1h**); this gives rise to an *epimerization* process. Two other pathways comprise the concurrent reversal of two propellers (**2h**); this leads to a *diastereomerization* process. The remaining two pathways involve the simultaneous reversal of three propellers (**3h**) to give an *enantiomerization* (**e**). The enantiomerization of isomers with C_2 symmetry—interconversion among the (M,M,P)-**1** and (P,P,M)-**1** stereoisomers—is worth noting, since it might occur either through the **3h** pathway or by way of the **1h** path due to symmetry reasons. Relying upon previous experimental results obtained for the homologous perchlorinated triphenylmethyl diradical **5** with two propeller subunits (Ar_2C^*Ar' , C^*Ar_2) that share the central aromatic Ar' ring,^[15] we assume from now on that the **1h** pathway is the most probable process for the interconversion between the C_2 and D_3 diastereomers of **1**.

The diastereomerization rates of **1** were determined in the range 292.5 to 320.5 K starting from THF solutions of the pure C_2 isomer and measuring the evolution against time of the

molar fractions of both diastereomers (Figure 3). A linear plot of $\log(\bar{k}/T)$ vs. $1/T$ was used to calculate $\Delta H^\ddagger = 90 \pm 2 \text{ kJ mol}^{-1}$ and $\Delta S^\ddagger = -34 \pm 6 \text{ JK}^{-1} \text{ mol}^{-1}$ ($\Delta G^\ddagger_{303 \text{ K}} = 100 \pm 2 \text{ kJ mol}^{-1}$) for the $C_2 \rightarrow D_3$ conversion (\bar{k} = overall rate constant for the isomerization of $C_2 \rightarrow D_3$).^[16]

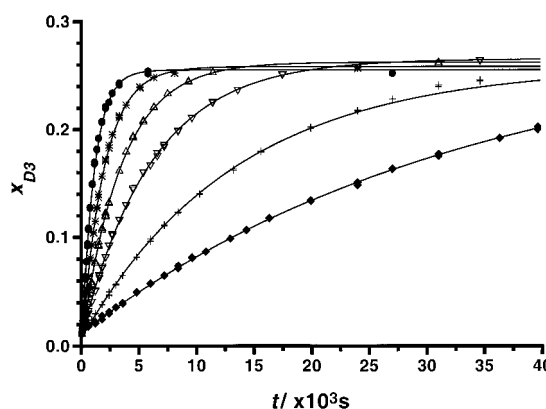


Figure 3. Kinetics of the isomerization of pure C_2 diastereomer of quartet **1** measured in THF at 293 (\blacklozenge), 298 ($+$), 306 (\blacktriangledown), 310 (\blacktriangle), 315 ($*$), and 321 K (\bullet). Continuous lines are the least-squared fits of experimental molar fractions (x_{D_3}) of the D_3 isomer to Equation (12).

The diastereomerization barrier for quartet **1** is very close to those found for the enantiomerization of perchlorotriphenylmethyl radical **4**, $\Delta G^\ddagger_{303 \text{ K}} = 98 \text{ kJ mol}^{-1}$, and for the diastereomerization of the perchlorinated diradical **5**,^[15] $\Delta G^\ddagger_{303 \text{ K}} = 98.3 \text{ kJ mol}^{-1}$; this confirms the initial assumption that the $C_2 \rightarrow D_3$ conversion takes place through an uncorrelated reversal of the helicity of one of its propeller-like subunits, that is, by a **1h** pathway. This behaviour can be explained on the basis of independent torsional motions of each Ar_2C^*Ar' subunit, which indicates that such torsional motions are mainly governed by the steric congestion that originates from the bulky chlorine atoms present inside this subunit. The development along time of the molar fraction of both isomers also allowed us to determine the effective equilibrium constant, $K = [D_3]_{\text{eq}}/[C_2]_{\text{eq}}$ for the $C_2 \rightleftharpoons D_3$ process in the temperature range of 292.5–320.5 K. A van't Hoff plot of the resulting effective equilibrium constants was used to calculate the thermodynamic parameters associated with the diastereomerization equilibrium of **1** in THF: $\Delta H^0 = -7.0 \pm 0.5 \text{ kJ mol}^{-1}$ and $\Delta S^0 = -31.1 \pm 1.5 \text{ JK}^{-1} \text{ mol}^{-1}$ ($\Delta G^\circ_{303 \text{ K}} = +2.5 \pm 0.5 \text{ kJ mol}^{-1}$). Such thermodynamical data indicate that the equilibrium is entropically controlled and that the ΔH^0 and ΔS^0 values found differ from those calculated or estimated theoretically, that is, $\Delta H^0_{\text{calcd}} = +1.7 \text{ kJ mol}^{-1}$ and $\Delta S^0_{\text{calcd}} = -9.1 \text{ JK}^{-1} \text{ mol}^{-1}$ (see below). It is worth noting the difference that exists in the estimated and observed ΔS^0 values. Entropy changes can be estimated for rigid molecules by the distinct rotational degrees of freedom of each isomer, which are given by the molecular symmetry. Therefore, the contribution of the symmetry to the entropy is $-R \ln \delta$, in which R = gas constant and δ is the symmetry number, that is, $\delta = 2$ and 6 for C_2 and D_3 , respectively.^[17] Under such circumstances it can be estimated that $\Delta S^0(C_2 \rightarrow D_3) = R \ln 1/3 = -9.1 \text{ JK}^{-1} \text{ mol}^{-1}$. The mismatching between this

value and that obtained experimentally suggests that additional entropic terms coming from the distinct interactions of both diastereomers with the solvent (THF) contribute to the equilibrium. Such a differential solvation of C_2 and D_3 isomers was experimentally confirmed later on. In fact, the thermodynamic parameters, which correspond to the $C_2 \rightleftharpoons D_3$ equilibrium, measured in another five media (see below) differ from each other depending on the solvent nature.

Differential chromatographic retention of diastereomers: As already mentioned, the diastereomers of quartet **1** can be separated by HPLC under reversed-phase conditions with octadecyl polysiloxane (ODS) as stationary phase and mixtures of CH_3CN and THF as the mobile phase.^[5] Retention times of both isomers show a marked dependence on the composition of the mobile phase. Thus, when pure THF or THF/ CH_3CN mixtures with percentages of CH_3CN below 50% were used, both isomers were unretained. However, when the percentage of CH_3CN is increased above 50%, the retention times grow and the rate of increase is faster for the D_3 isomer. This differential behaviour is depicted in Figure 4, in which the variation of the capacity factors (k'_i) of both isomers versus the percentage of CH_3CN in the mobile phase is shown.^[18]

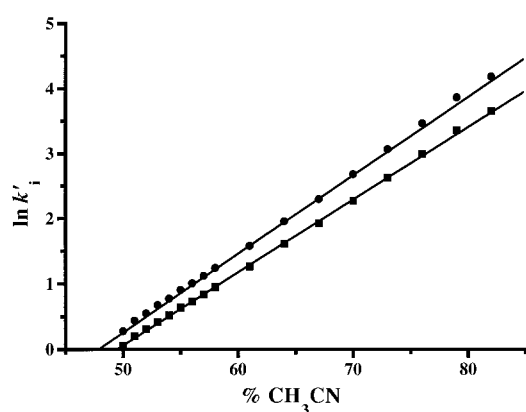


Figure 4. Dependence of the capacity factors (k'_i) of isomers C_2 (■) and D_3 (●) of quartet **1** on the volumetric composition (in %) of CH_3CN of the THF/ CH_3CN mixtures used as mobile phases of the chromatographic separations.

Temperature has also a noticeable influence on the retention times and the separation factor (α) of both diastereomers.^[19] In Figure 5, we show the chromatographic resolutions achieved in the temperature range of 288–318 K, with the composition of the mobile phase ($\text{CH}_3\text{CN}/\text{THF}$) kept constant in all cases at 60:40. In decreasing the temperature, the retention times of both isomers increases, although the retention of the more strongly retained isomer, the D_3 one, decreases at a greater rate than that of the C_2 isomer. Thus, the magnitude $\ln \alpha$ drops as the temperature decreases in the range of 288–318 K.

This temperature effect is the usual one for a “regular” or “enthalpy/entropy-compensated” chromatographic separation, which suggests that the retention of each isomer in the

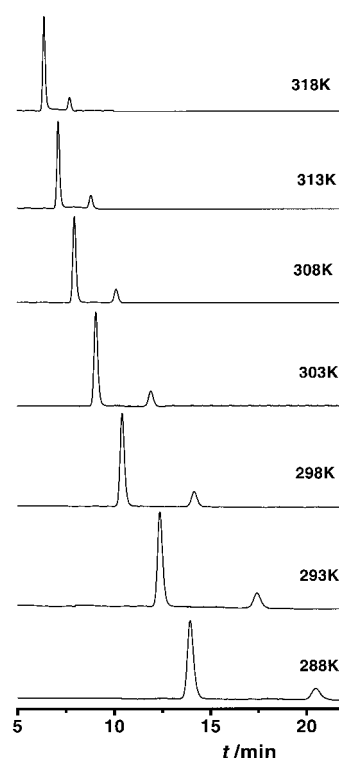


Figure 5. Chromatographic resolutions of isomers C_2 and D_3 of quartet **1** achieved in the temperature range of 288–318 K. Chromatographic conditions: Spherisorb ODS-2 (25×0.46 cm; $5 \mu\text{m}$ particle diameter); 1 mL min^{-1} ; mobile phase, $\text{CH}_3\text{CN}/\text{THF}$ (60:40); UV detection at $\lambda = 255 \text{ nm}$.

stationary phase is controlled by a single operative sorption mechanism and that this mechanism is the same for both isomers.^[20] Under such circumstances, the capacity factor of each isomer must be related [Eq. (2)] with the changes of standard molar enthalpies, $\Delta(\Delta H_i^0)$, and entropies, $\Delta(\Delta S_i^0)$, involved during the transfer of the solute from the mobile phase to the stationary one.

$$\ln k'_i = -\Delta(\Delta H_i^0)/RT + [\ln \phi + \Delta(\Delta S_i^0)/R] \quad (2)$$

In Equation (2) ϕ is the ratio between the volumes of the stationary, V_s , and the mobile, V_m , phases of the chromatographic system used in the experiment, that is, $\phi = V_s/V_m$. Moreover, there must be a linear dependence of $\Delta(\Delta H_i^0)$ on $\Delta(\Delta S_i^0)$, such as $\Delta(\Delta H_i^0)/\Delta(\Delta S_i^0) = T_\beta/1000$, in which the so-called isoequilibrium temperature (T_β) is independent of the isomer. In accordance with Equation (2), the plots of $\ln k'$ versus $1/T$ for the two diastereomers of quartet **1** appear to be linear in the temperature range studied ($r^2 = 0.998$ and 0.999); this confirms the previous suggestion that a single sorption mechanism is operative for both isomers. These plots also permit us to calculate $\Delta(\Delta H_i^0)$ and $\Delta(\Delta S_i^0)$ values for both isomers, which are $-29.5(2) \text{ kJ mol}^{-1}$ and $-85(1) \text{ JK}^{-1} \text{ mol}^{-1}$, respectively, for the D_3 isomer, and $-25.2(2) \text{ kJ mol}^{-1}$ and $-74(1) \text{ JK}^{-1} \text{ mol}^{-1}$, respectively, for the C_2 one. Interestingly, both isomers have the same isoequilibrium temperature, $T_\beta = 344(7) \text{ K}$, which indicates that they have the same retention mechanism, although the strengths of solute/solvent interactions are different for both isomers.

Linear solvation free-energy relationship: To better define and understand the common retention mechanism that governs the differential chromatographic retention of the isomers of **1**, as well as the origin of the differential retention for both diastereomers, a complete study assessing all the possible intermolecular forces was required. For this objective, we used the linear solvation free-energy relationship (LSER) quantitative treatment, which was developed previously by Kamlet, Taft, and co-workers.^[21] Such a treatment had previously been used successfully by Sadeck et al. in describing the partitioning of solutes in HPLC.^[22] LSER assumes that the different solvent/solute interactions are additive and can be categorized in two groups: the exoergic and endoergic interactions.^[23] The exoergic interactions have their origins in attractive solute/solvent interactions and can be quantified by the solvatochromic parameters π^* , α , and β . These parameters are determined by UV/Vis spectroscopic measurements and can be classified in nonspecific (π^*) and specific (α and β) parameters. The π^* parameter measures the exoergic effects of dipole/dipole and dipole/induced dipole interactions between the solute and solvent molecules. The solvatochromic parameter α is a quantitative empirical measure of the ability of a bulk solvent to act as hydrogen-bond donor toward a solute. By contrast, the empirical parameter β measures quantitatively the ability of a bulk solvent to act as a hydrogen-bond acceptor or electron-pair donor toward a given standard solute. Finally, we have to consider the endoergic term, named cavitation term (Ω). This term measures the work required for separating the solvent molecules to provide a suitable sized and shaped enclosure in which the solute molecule can be accommodated. The Ω term represents the physical quantity of cohesive pressure—or cohesive energy density—of the solvent. This quantity is the square of the Hildebrand's solubility parameter, δ_H , which is given by $\delta_H = (\Delta H^0 - RT/V_m)^{1/2}$, in which ΔH^0 is the molar standard enthalpy of vaporization of the solvent to a gas of zero pressure, and V_m is the molar volume of the liquid solvent. Therefore, the generalized LSER that describe the transfer of a solute from the mobile to the stationary phase in chromatographic separations, performed at a constant temperature and changing the composition of the mobile phase, adopts the form of Equation (3) for a series of solutes i .^[23]

$$\ln k'_i = e'_i + s'_i \pi^* + a'_i \alpha + b'_i \beta + m'_i \Omega \quad (3)$$

In Equation (3) s'_i , a'_i , b'_i , and m'_i are coefficients that are characteristic of each solute i and independent of the nature of the stationary and mobile phases. Such coefficients must have negative (or positive) signs accordingly with the exoergic (or endoergic) nature of each term. Finally, the independent term e'_i depends on the nature of the solute and the mobile and stationary phases as well as the temperature. For this study, we simplified Equation (3) by eliminating the fourth term ($b'_i \beta$), since **1** does not have any hydrogen-bond donor ability.

For chromatographic separations in which the mobile phase composition is maintained constant but the temperature changes, the LSER described by Equation (3) must be slightly

modified. Temperature changes not only affect the mobile phase but also the stationary phase and, consequently, they must be taken into account. Therefore, in this case the generalized LSER is given by Equation (4), in which $\pi^*(T)^{s/m}$, $\alpha(T)^{s/m}$, $\beta(T)^{s/m}$, and $\Omega(T)^{s/m}$ are the differences between the parameters corresponding to the mobile and stationary phases at a given temperature T , namely, $\Omega(T)^{s/m} = \Omega(T)^s - \Omega(T)^m$.

$$\ln k'_i = e_i^{s/m} + s_i \pi^*(T)^{s/m} + a_i \alpha(T)^{s/m} + m_i \Omega(T)^{s/m} \quad (4)$$

In this generalized LSER, the β term, which takes into account the hydrogen-bond acceptor ability of solvents, is neglected, since **1** does not have any H atoms. Coefficients $e_i^{s/m}$, s_i , a_i , and m_i of Equation (4) have their usual meaning and their signs must be opposed to those of Eq. (3), which in this case is positive (or negative) accordingly with the exoergic (or endoergic) nature of each term. The variables π^* , α , Ω , $\pi^*(T)^{s/m}$, $\alpha(T)^{s/m}$, and $\Omega(T)^{s/m}$ were experimentally determined by the usual procedures as described in the Experimental Section.

The capacity factors ($\ln k'_i$) of the C_2 and D_3 isomers, obtained at different temperatures and with distinct CH₃CN/THF percentages in the mobile phase, were fitted to the experimentally determined values for the cavitation and solvatochromic parameters by means of a multivariable linear regression method to the corresponding LSER expression. When the multiple regression was based in a physicochemical model that includes all the solvent strength parameters [i.e., complete Eqs. (3) and (4)] the fit was inadequate. They did not pass any of the usual statistical tests even at low confidence levels. Only models which included exclusively the independent and the cavity formation terms [i.e., the first and last terms of the right-hand sides of Eqs. (3) and (4)], and eliminate the dipolarity and the two hydrogen-bonding terms fit the data well. These models were valid at the 99.95% (F test) significance level ($F = 25.000$; $p < 0.0005$). Table 2 lists the resulting regression coefficients of such fits.

The resulting signs of the m_i and m'_i coefficients are negative and positive, respectively, as expected from the endoergic nature of the cavitation terms and the theoretical grounds of Equations (3) and (4). Up to now, we have shown that the most important solvent parameter that influences the differential chromatographic retention of the diastereomers of **1** is the cavitation parameter Ω . Consequently, any

Table 2. Linear Solvation Free Energy Relationships describing the HPLC chromatographic retention of the diastereomers of quartet **1** changing a) the CH₃CN/THF mobile phase composition, and b) the temperature of the chromatographic experiment. a) Physicochemical model: $\ln k' = e'_i + m'_i \Omega$. b) Physicochemical model: $\ln k' = e_i^{s/m} + m_i \Omega(T)^{s/m}$

Coefficients				
a)	e'_i	m'_i	$r^{[a]}$	$N^{[b]}$
C_2	-24.6	30.1	0.999	10
D_3	-26.5	32.5	0.999	10
b)	$e_i^{s/m}$	m_i	$r^{[a]}$	$N^{[b]}$
C_2	-8.4	-14.8	0.999	8
D_3	-9.6	-17.2	0.999	8

[a] Correlation coefficients. [b] Number of data points.

temperature or mobile phase composition change that causes an increase of the required energy to form a cavity in the mobile phase produces an increase of the retention time for both isomers, since the transfer to the stationary phase is energetically favored. It is also expected that an increase of the A_{MS} of the solute will require more energy to form the cavity in the mobile phase. Therefore, the isomer with a higher A_{MS} will be more sensitive to any change in the cavitation parameter and the retention time will increase. For compound **1**, the absolute values of coefficients m_i and m'_i are larger for the D_3 isomer than for the C_2 one; this indicates that the first one is more sensitive to the cavity formation process. This result is in agreement with the lower fractal dimension and larger molecular surface area of the D_3 isomer. Therefore, it can be concluded that the texture or roughness is one of the most important structural characteristics of the diastereomers of quartet **1** for their chromatographic discrimination.

Equilibrium of diastereomerization: The results from the experiments described above pointed out that the differential chromatographic retention of the diastereomers of **1** is mainly governed by the differences in their molecular surfaces and shapes. Nevertheless, these experiments are somewhat limited, since in the ranges assayed of mobile-phase composition and temperature the solvatochromic parameters α and π^* remain nearly constant. Thus, such experiments do not provide too much information about solute/solvent interactions through hydrogen bonds or dipolarity/polarizability interactions. Therefore, we moved on to the study of another physicochemical property that could be influenced by all kinds of solute/solvent interactions. For this purpose, we chose the influence of solvent effects on the equilibrium constant of $C_2 \rightleftharpoons D_3$. Two different experiments, focused on the study of the influence of solvent nature on this equilibrium, were carried out. Initially, variations of the equilibrium constant (K) at different temperatures for six representative solvents were studied. These variations, shown in Figure 6, were determined in the temperature range of 305–340 K by measuring the relative proportion of both isomers by analytical HPLC. Under such conditions, the changes of K can be

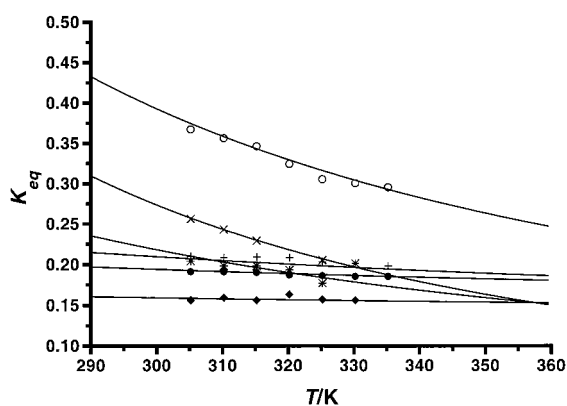


Figure 6. Temperature dependence of the equilibrium constant (K) of the $C_2 \rightleftharpoons D_3$ process for six representative solvents: (○) THF, (×) nC_6H_{14} , (+) $CHCl_3$, (*) CH_3CN/THF , 60:40, (●) $C_6H_5CH_3$, and (◆) C_6H_6 . Continuous lines are the least-squared fits of experimental data to Equation (5).

correlated with the changes in the standard molar enthalpies ΔH_i^0 and entropies ΔS_i^0 by Equation (5).

$$K = \exp(-\Delta H_i^0/RT + \Delta S_i^0/R) \quad (5)$$

The resulting changes of ΔH_i^0 and ΔS_i^0 are given in Table 3. It is interesting to see that an extra thermodynamic relationship exists between the ΔH_i^0 and ΔS_i^0 changes in different solvents, i.e., $\Delta(\Delta H_i^0) = T_c \Delta(\Delta S_i^0)/1000$ with a compensation temperature of $T_c = 354$ K. As in the case of the differential chromatographic retention of the stereoisomers such a behaviour indicates that the diastereomerization process is mostly controlled by a single mechanism.^[24]

Table 3. Thermodynamic parameters corresponding to the diastereomerization equilibrium of quartet **1** in six different solvents.

	$K_{305}^{[a]}$	ΔH_i^0 ^[b] $D_3 \rightarrow C_2$	ΔS_i^0 ^[c] $D_3 \rightarrow C_2$	ΔG_{305K}^0 ^[b] $D_3 \rightarrow C_2$	$r^{[d]}$
THF	0.367	-7.0 ± 0.5	-31.1 ± 1.5	2.5 ± 0.9	0.971
nC_6H_{14}	0.256	-9.0 ± 0.3	-40.8 ± 1.1	3.4 ± 0.7	0.995
$CHCl_3$	0.210	-1.8 ± 0.3	-19.0 ± 1.1	4.0 ± 0.7	0.850
$C_6H_5CH_3$	0.191	-1.1 ± 0.1	-17.3 ± 0.4	4.2 ± 0.2	0.936
C_6H_6	0.156	-0.6 ± 0.4	-17.3 ± 1.2	4.7 ± 0.8	0.943
CH_3CN/THF ^[e]	0.204	-5.5 ± 0.6	-31.1 ± 2.0	4.0 ± 1.2	0.915

[a] Equilibrium constants at 305 K. [b] In kJ mol^{-1} . [c] In $\text{J mol}^{-1} \text{K}^{-1}$. [d] Regression coefficients of van't Hoff plots. [e] Volumetric composition of 60/40.

The second experiment was designed to provide some insight into the nature of this single mechanism, that is, to investigate the different kinds of interactions between the diastereomers of **1** and their surroundings. In this experiment, the equilibrium constant was determined at a given temperature of 310 K, measuring the relative proportion of both isomers by HPLC in a series of solvents considered as representative of all possible types of solute/solvent interactions. In order to select this set of representative solvents, we performed (see Appendix) a classification of the most common organic solvents in eleven different groups, named groups A–K, and choose 19 different solvents belonging to seven of such groups. Unfortunately, solvents of the F, I, J, and K groups could not be used as a result of the low solubility of quartet **1** in such solvents.

Linear solvation free-energy relationship: To determine the nature of the interactions controlling the diastereomerization process, a physicochemical model derived from an LSER was used to fit the equilibrium constants, which were obtained experimentally at 310 K for each of the studied solvents. The generalized model that describes the isomerization process adopts the form of Equation (6).

$$\ln K(S_e, T_e) = e + a\alpha(S_e, T_e) + s[\pi^*(S_e, T_e) + d\delta(S_e, T_e)] + m\Omega(S_e, T_e) \quad (6)$$

In this expression $\alpha(S_e, T_e)$, $\pi^*(S_e, T_e)$, $\delta(S_e, T_e)$, and $\Omega(S_e, T_e)$ are the descriptive solvatochromic and cavitation parameters of the solvent S_e at a temperature of $T_e = 310$ K, and $K(S_e, T_e)$ is the diastereomeric equilibrium constant in this

solvent at such a temperature. These parameters are abbreviated as α , π^* , δ , and Ω for simplicity. The independent term e represents the logarithm of the equilibrium constant at 310 K in the absence of any dipolar and hydrogen-bond interaction and any cavitation effect. The solvatochromic β and ζ parameters were not considered in Equation (6), since none of the isomers of **1** has hydrogen-bond donor or basic properties. To fit the experimental values of $K(S_e, 310)$ and those of solvatochromic parameters to Equation (6), a multi-variable linear regression was used.^[25] The regression model for this fit was found to be valid at a significance level $\alpha \geq 99.9\%$ with a correlation coefficient of 0.849. After an exhaustive analysis of the residual errors, we realized that two of the solvents (THF and CCl_4) were out of the regression.^[26, 27] Therefore, in a second fit these two solvents were removed and the significance level and the correlation coefficients were considerably improved (see Table 4). In addition, the signs of the different coefficients were maintained constant in both fits, confirming the robustness of the regression model.

The signs of the different coefficients agree with those theoretically expected, considering the *endo*- and *exoergic* nature of the respective terms and the structural and electronic characteristics of both isomers. Indeed, the signs of the s and d' ($d' = s \times d$) coefficients are negative, indicating that an increase of the solvent polarity shifts the equilibrium from the D_3 isomer ($\mu = 0$) towards the C_2 isomer, in accordance with its small dipole moment. The sign of the m coefficient is also negative, showing that an increase of the solvent cavitation parameter shifts the equilibrium in the same direction. This result is in agreement with the smaller A_{MS} of the C_2 isomer. On the other hand, the a coefficient is positive, which indicates that an increase of the ability of the solvent to act as a hydrogen-bond donor shifts the equilibrium towards the D_3 isomer. This displacement also agrees with the fact that the chlorine atoms of the D_3 isomer are more accessible to interact with the solvent molecules owing to its less cleaved and more open structure. Special attention is also focused on the independent or intercept term, e . This term measures the equilibrium constant of the process at 310 K in absence of any solute/solvent interactions and, therefore, it can be considered in a first approximation as the equilibrium constant at 310 K in vacuum, that is, $e = \ln K(\text{vac}, 310)$. This equilibrium constant is related to the differences in the molar standard enthalpies, $\Delta(\Delta H^0)$, and entropies, $\Delta(\Delta S^0)$, of formation of both isomers through Equation (7). Hence, it is possible to estimate $\Delta(\Delta H^0)$, taking into account the value for $\Delta(\Delta S^0)$, which is calculated from the contributions of the

molecular rotational degrees of freedom. Thus, the resulting relative stability of the isomers is $\Delta(\Delta H^0) = \Delta H^0(D_3) - \Delta H^0(C_2) = -1.5 \pm 0.5 \text{ kJ mol}^{-1}$. This small difference is in accordance with the similar enthalpies found for both isomers from AM1 semiempirical calculations.

$$\Delta(\Delta H^0) = -RT \ln K(\text{vac}, 310) + T \Delta(\Delta S^0) \quad (7)$$

Finally, relative contributions of the various solute/solvent interactions for the diastereomerization process of quartet **1** is shown in Figure 7. These results show that the displacement of the diastereomeric equilibrium of quartet **1** is firstly controlled by the modifications in the cohesiveness of the

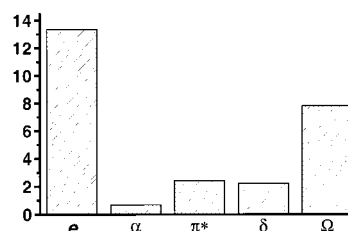


Figure 7. Relative contributions of solute/solvent interactions to the equilibrium of diastereomerization of **1**. Columns, marked by α , π^* , δ , and Ω , represent the cumulative contributions of hydrogen-bond and dipolarity/polarizability interactions and cavitation effects, respectively, for all studied solvents. The bar marked by e represents the relative contribution from the equilibrium constant of the process at 310 K in absence of any solute/solvent interaction.

surrounding medium, followed by the dipolarity/polarizability changes, and finally by the hydrogen-bond interactions. Therefore, once again it has been confirmed that the difference in shape and molecular surface of both isomers of **1** are among the most relevant molecular characteristics that control their different physicochemical properties.

Tumbling processes of the diastereomers: Up to now, we have shown that the difference in physicochemical behaviour of the isomers of quartet **1** is mainly controlled by the differences in their molecular shapes and fractalities as well as by the cohesiveness of the solvent. Nevertheless, in order to provide a complete description of the rest of solute/solvent interactions, we studied the molecular tumbling of both isomers inside solid or viscous amorphous matrices, since this process should not depend on the creation of cavities inside the solvent matrix. ESR spectroscopy is the most suitable technique for studying such a dynamic process because of

Table 4. Linear Solvation Free Energy Relationship describing the $C_2 \rightleftharpoons D_3$ process at 310 K for quartet **1** in nineteen different solvents. Physicochemical model: $\ln K(S_e, 310) = e + s\pi^* + d'\delta + a\alpha + m\Omega$

Fit no.	$n^{[a]}$	$N^{[b]}$	Coefficient (t test) ^[c]						Statistics				
			E	s	$d'^{[d]}$	a	$m^{[e]}$	r	s	r^2	F	p	
1	19	14	-0.8(2.6)	-0.3(0.9)	-0.4(2.5)	0.4(0.8)	-0.6(1.1)	0.849	0.216	0.642	9.067	≤ 0.001	
2	17	12	-0.8(4.2)	-0.3(1.3)	-0.3(3.0)	0.7(1.9)	-0.7(2.0)	0.931	0.138	0.821	19.390	≤ 0.0005	

[a] Number of data points. In fit no. 2 the solvents THF and CCl_4 were eliminated. [b] Degrees of freedom. [c] Number in parentheses is the student's test value for the coefficient. [d] Coefficient d' is related with those of Equation (6) by $d' = sd$. [e] Cavitation parameters were divided by 100 to keep their values in the same range as the other parameters.

the open-shell character of both diastereomers. Moreover, the experimental timescale of this technique lies in the range of the orientation/motion correlation times (τ) of tumbling processes for most organic molecules.

ESR spectra of high-spin molecules display fine structures with several turning points and singularities due to the anisotropy of the magnetic dipolar interactions between the unpaired electrons; these are quantified by the zero-field-splitting (ZFS) parameters D' and E' . Such a fine structure can be washed out if the anisotropic interactions are averaged out by a fast tumbling of molecules. Therefore, changes in the fine structure provide information about this dynamic process. Figure 8 depicts the first-derivative ESR spectra of the D_3 isomer measured in benzene in the temperature range of 110–270 K, in which striking changes are noticed.

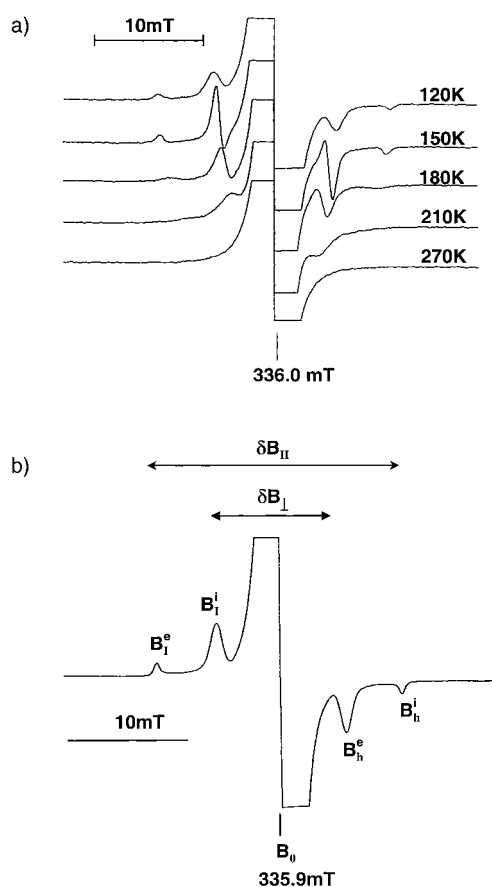


Figure 8. ESR spectra of the D_3 isomer of quartet **1**. a) Selected spectra in different motion regions: spectra in benzene at the temperature range of 120–270 K. b) Rigid-limit region: spectrum in nC_6H_{14} at 110 K showing the extreme turning points at magnetic fields of B_i^e and B_h^e , the intermediate divergence points at magnetic fields of B_i^i and B_h^i , and the central line at B_o .

The observed changes in these spectra are typical of the line-shape effects produced by the reorientation motion of quartets.^[28] Thus, in the rigid-limit region, that is, at temperatures below 120 K, the spectra correspond to those expected for an ensemble of randomly oriented rigid quartets with axial symmetry. They show two extreme turning points or steps at constant low (B_i^e) and high (B_h^e) magnetic fields, two intermediate divergence peaks at fields of B_i^i and B_h^i , and also an intense symmetrical central line at the magnetic field

of B_o .^[29] When the sample temperature increases above 120 K, the rigid-limit ESR spectrum changes its overall lineshape as a result of the dynamic line broadening and the motional averaging of the anisotropic part of the inhomogeneous line broadening. Thus, the two extreme steps and the two divergence peaks of the fine-structure spectrum shift gradually toward the central line, which results in a decrease in the separations between the above-mentioned spectroscopic features, that is, a decrease of $\delta B_{\parallel} = B_h^e - B_i^e$ and $\delta B_{\perp} = B_h^i - B_i^i$ is observed. These changes occur in the temperature range 130–195 K and are typical of the line-shape effects in the so-called *region of slow-tumbling motion*, for which the correlation times (τ) are larger than the spin–spin relaxation times (T_2), that is, $\tau \gg T_2$. At higher temperatures, the dynamic line broadening and line shift are such that extreme steps are largely masked by the divergence peaks and the last ones severely overlap with the central line. It can also be seen from Figure 8, that the extreme steps shift towards the central line at a faster rate than the divergence peaks, while the linewidth of the central line gradually decreases. Consequently, in the temperature range from 200 to 250 K, the observed spectra consist of an intense line with two structured shoulders on both sides, which move toward the central line as the sample temperatures increases. This temperature range represents the *region of intermediate-tumbling motion*, where $\tau \approx T_2$. In the vicinity of 250 K, the spectra display a single, symmetric line due to a complete motion shift the spectral features; this indicates the beginning of the *region of fast-tumbling motion* for which $\tau \ll T_2$. In this region at high enough temperatures, the motion-independent anisotropic contribution to the inhomogeneous line broadening should vanish, and the residual line should correspond to the motion-independent isotropic contribution. Thus, the spectra in this region, not depicted in Figure 8, consist of a unique symmetric, single central line in which its peak-to-peak linewidth decreases with increasing temperature due to dynamic narrowing by the fast-tumbling motion.

Lee et al. evolved a comprehensive analytical/theoretical treatment for explaining such ESR spectral changes, based on the solution of differential equations for the reorientational isotropic diffusion for an ensemble of high-spin systems under motion.^[28] These authors obtained an analytical expression [Eq. (8)] for the region of slow-tumbling motion that relates the orientation/motion correlation time τ (in s), or the corresponding tumbling rate τ^{-1} , with the step separation δB_{\parallel} of the ESR fine-structure of a quartet.

$$\tau = \frac{1.92756 \times 10^{-7} D'}{[4D' - \delta B_{\parallel}]^2} \quad (8)$$

In Equation (8) D' is the absolute value of the zero-field-splitting parameter of the quartet, given in Gauss. We have used this equation to determine the tumbling rates of the stereoisomers C_2 and D_3 in C_6H_6 and nC_6H_{14} , in the temperature range corresponding to the region of slow-tumbling motion. The plots of $\ln(\tau^{-1})$ versus $1/T$ allowed us to calculate, by means of the Arrhenius equation, the activation energies (E_a) for the tumbling processes of both isomers; these are given in Table 5. The E_a values in C_6H_6 are larger than in

Table 5. Activation energies (E_a) and preexponential factors, A , associated to the tumbling processes of the C_2 and D_3 isomers of quartet **1** in frozen matrices of n -hexane and benzene.^[a]

Solvent	Diastereomer	E_a ^[b]	$\ln A$
n -hexane	C_2 ^[c]	29 ± 3	41 ± 2
	C_2 ^[d]	26 ± 2	38 ± 2
	D_3 ^[c]	20 ± 1	34 ± 1
	D_3 ^[d]	21 ± 1	35 ± 1
benzene	C_2 ^[c]	34 ± 2	40 ± 2
	C_2 ^[d]	35 ± 5	42 ± 3
	D_3 ^[c]	24 ± 1	34 ± 1
	D_3 ^[d]	22 ± 3	33 ± 2

[a] The correlation coefficients of the different fits were $r^2 = 0.93 - 0.99$.

[b] In kJ mol^{-1} . [c] Results obtained from samples consisting of diastereomeric mixtures. [d] Results obtained from pure samples of both isomers.

nC_6H_{14} for both isomers, and the values for the D_3 isomer are always larger than those obtained for the C_2 one, regardless the nature of the solvent. Both trends agree with those theoretically expected if the reorientation motions of quartets inside the cavities are mainly limited by the dipolar interactions. Actually, the polarity of C_6H_6 is somewhat higher than that of nC_6H_{14} and the dipole moment of the D_3 isomer is zero, while that of C_2 is nonzero. Therefore, it can be concluded that in the absence of any cavitation effect the dipolarity/polarizability effects control the different tumbling rates of the two isomers.

Summary and Conclusion

In summary, we have demonstrated experimentally that the different molecular surface area and fractal dimensionality of the diastereomers of a rigid molecule are among the most important molecular parameters controlling some of their physicochemical properties. In particular, we have observed that the difference in chromatographic retention of the two diastereomeric forms of a quartet molecule and the equilibrium between these isomers are strongly influenced by these molecular parameters. These results were obtained by employing the *linear solvation free-energy relationship* (LSER) approach to experimental data, for which the cavitation effect, the dipolarity/polarizability, and the hydrogen-bonding ability of the solvent were considered to be the most important solute/solvent interactions. In order to use such an LSER approach efficiently, a general classification of classical organic solvents in eleven different categories has been carried out. The results of this study demonstrate that the shape and roughness (fractality) of the diastereomers are among their most important molecular characteristics in relation with their ability to interact with the surrounding media, mainly as a result of cavitation effects. In contrast, when these effects are not important, as with the tumbling of the isomers inside the preformed cavities of the solvent, the unique molecular parameter that discriminates the behavior of both stereoisomers seems to be the dipolarity/polarizability. We are currently working to extend these studies to other kinds of molecules including second-generation dendrimers such as **2**.

Appendix

General classification of organic solvents for LSER studies: One of the major difficulties in the study of any free-energy-based physicochemical process (or property) by means of an LSER approach is to choose a proper series of solvents that can be considered as representative of all kinds of different solute/solvent interactions. This selection is usually performed based on the previous experience and chemical intuition; however, to our knowledge, a general procedure for such a solvent selection does not exist. One systematic and efficient way to carry out such a choice would be to collect all the most common organic solvents together in a limited number of groups, in such a way that each group contains all solvents that have the same type of interactions with similar magnitudes. Thus, a set of solvents composed by one or two members of each of these groups would be representative of all kind of interactions, since it should manifest a considerable variation of all solvent properties. Here, we present one of such general classification that can be useful for any kind of LSER study. As already explained, the principal solute/solvent interactions that govern any free-energy-based physicochemical property are the following: the dipolarity/polarizability, described by the π^* scale and its correction parameter δ , the ability to give or accept hydrogen bonds, represented by the α and β solvatochromic parameters, respectively, and the difficulty to create a cavity inside the solvent, quantified by the Ω cavitation parameter.^[23] In the study of basic properties of a solute, it is also necessary to include the ζ solvatochromic parameter, which measures the effect of the different atoms of the solvent which interact with the lone pair of electrons of the solute.

In order to perform this general classification, the most common organic solvents (47 solvents listed in Table 6) were initially chosen and grouped in the six-dimensional space defined by the six solvent parameters previously described, that is, α , β , π^* , δ , ζ , and Ω . We then applied a principal component analysis (PCA) to reduce the dimensions of this space, while keeping constant the maximum of the original information of all the population studied.^[30] All the calculations relative to the PCA, the graphic representations, and the hierarchical classification were performed with the ESTATS and PARVUS programs.^[31, 32] First, the matrix of the original solvent data (\mathbf{X}), composed of 47 rows and six columns, was treated in order to autoscale all the experimental values of the solvatochromic and cavitation parameters. Then, the principal components were calculated from the pre-treated matrix (\mathbf{X}'), by the diagonalization of the variance/covariance matrix between the different variables to give their *eigenvalues* (λ_j) and *eigenvectors* (b_j). The eigenvalues of each principal component show the rate of variance (dispersion) for that component, meanwhile the eigenvectors give information about the coefficients of the linear combination of the original variables (parameters) that define the principal component. It can be concluded that the original six-dimensional space can be reduced to a new three-dimensional space, defined by three principal components (PC_1 , PC_2 , PC_3). These principal components are a linear combination of the original six solvent parameters and still contain unaltered almost the 80% of the original information of the whole studied population.

Two "loading" representations, which correspond to the projection of the variable (parameters) over the principal components are shown in the insets of Figure 9. An analysis of these data confirms that α and Ω are the principal parameters for the first principal component (PC_1), π^* and δ are the more relevant ones for the second principal component (PC_2), and finally δ and ζ are the relevant parameters for the third principal component (PC_3). Once the 47 solvents were considered in this new three-dimensional space, the coordinates [PC_{1i} , PC_{2i} , PC_{3i}] of each solvent (i) in that new space are calculated by substitution of the values of the parameters (variables) of each solvent in the linear combinations which define each principal component.

In order to cluster the 47 solvents in different groups in the three-dimensional space (Figure 9), a hierarchical classification has been done over the solvents by using the Euclidean distance as a similarity criterion. Then, two solvents are more similar as the distance between them in the considered space is smaller.^[33] The number of groups depends upon the maximum distance allowed to be able to belong to the same cluster. In the present work, the distance between the $C_6H_5CH_3$ and CCl_4 has been considered as the discriminatory one. Following that criterion, the 47 solvents were clustered in eleven different groups which are designated

Table 6. General classification of 47 organic solvents in eleven groups named by letters A–K. Description of each group is performed by the mean value of the solvatochromic and cavitation parameters corresponding to the solvents grouped in this group.

Solvents ^[a]	α_m	β_m	π_m^*	Ω_m	δ_m	ζ_m
A <i>n</i> -hexane (1) <i>c</i> -hexane (2)	0.000	0.000	−0.040	57.453	0.000	0.000
B diisopropyl ether (3) di- <i>n</i> -butyl ether (4) diethyl ether (5) di- <i>n</i> -propyl ether (11)	0.000	0.470	0.263	53.259	0.000	0.200
C 1,4-dioxane (6) 1,2-dimethoxyethane (10) tetrahydrofuran (7) tetrahydropyran (9) anisole (8) acetonitrile (27) 2-butanone (12) <i>c</i> -hexanone (14) ethyl acetate (16) ethyl chloroacetate (17) methyl acetate (18) methyl formate (19) ethyl formate (20) acetone (13) <i>c</i> -pentanone (15)	0.023	0.424	0.642	91.091	0.000	0.080
D toluene (29) benzene (30) chlorobenzene (31) bromobenzene (32)	0.000	0.085	0.658	85.607	1.000	0.000
E tetrachloromethane (33) tetrachloroethene (39) trichloroethene (34) 1,1,1-trichloroethane (35) 1,2-dichloroethane (36) 1,2-dibromoethane (40) dichloromethane (37) trichloromethane (38) 1,2-dichloro- <i>E</i> -ethene (41)	0.082	0.000	0.553	84.454	0.500	0.000
F dimethylsulfoxide (24) <i>N,N</i> -dimethylformamide (22) <i>N,N</i> -dimethylacetamide (21)	0.000	0.737	0.920	138.922	0.000	0.000
G <i>tert</i> -butanol (42) <i>iso</i> -propanol (43) <i>n</i> -butanol (44) ethanol (45) methanol (46)	0.798	0.846	0.500	142.263	0.000	0.200
H nitrobenzene (25) benzotrile (26)	0.000	0.650	0.955	119.095	1.000	0.200
I pyridine (28)	0.000	0.640	0.870	107.653	1.000	0.600
J triethylamine (23)	0.000	0.710	0.140	53.005	0.000	1.000
K water (47)	1.170	0.180	1.090	537.811	0.000	0.200

[a] Numbers in parenthesis are numeral descriptors of solvents.

by the letters A–K and which are summarized in Table 6, together with all the mean values of their solvatochromic and cavitation parameters. Therefore, the selection of a series of solvents composed of one solvent of each of these eleven groups will be representative of all kinds of solute/solvent interactions and can be used in the study of any process (or property) by the LSER approach.

Experimental Section

General Methods: Reagents were obtained commercially from Fluka and Aldrich. Solvents for spectroscopic experiments were purchased as spectroscopic grade. Solvents for chromatographic experiments were obtained as super purity grade from Romil. THF and toluene were distilled in presence of benzophenone ketyl and of an excess of potassium metal

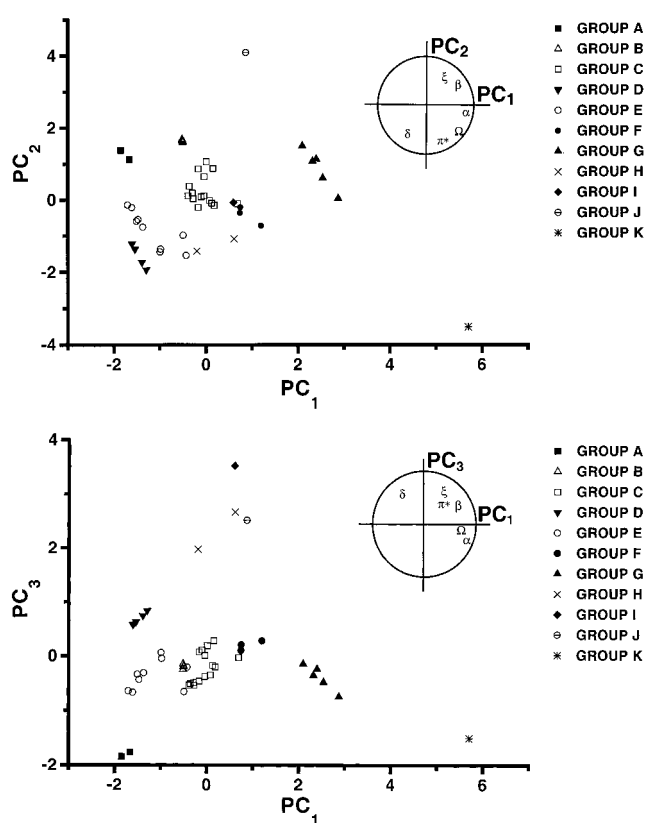


Figure 9. Projection of the 47 studied organic solvents in the space defined by the three principal components showing the hierarchical classification in eleven groups, named A–K. Top: PC_1 – PC_2 space. Bottom: PC_1 – PC_3 space. Insets: Loading representations showing the correlation between the α , β , π^* , δ , ζ , and Ω variables and the principal components.

under argon immediately before their use. Quartet **1** and its precursors were obtained as previously described.^[5] HPLC chromatography was performed on a Perkin–Elmer Series LC-235 spectrophotometer equipped with a diode array detector, a PE Nelson Series 900 interface coupled to an external computer, and a Perkin–Elmer Series 410 pump system. For the analytical HPLC experiments, a Spherisorb ODS-2 column (0.46 × 25 cm, 5 μ m particle size) was used as stationary phase, with a CH_3CN/THF (50:50) mixture with a flow rate of 1.0 mL min^{−1} as mobile phase. The column was thermostated at the different working temperatures with a glass homemade jacket equipped with an F3 Haake thermostat provided with an external circulator. Semipreparative HPLC was performed on a Spherisorb ODS-2 column (0.75 × 25 cm, 5 μ m particle size) with a flow rate of 5 mL min^{−1} of CH_3CN/THF (60:40), with the same equipment as reported for the analytical experiments. UV/Vis spectra were measured with a Varian Cary 05 spectrometer, provided with a multicell block, equipped with a temperature controller working in the range of 268–373 K. ESR spectra were recorded on an X-band Bruker ESP 300E spectrometer equipped with an ER4121 HT temperature controller. All precautions were taken into account to avoid undesirable spectral line broadening arising from microwave power saturation and magnetic-field over modulation. The samples were degassed three times by the freeze-(liquid N_2)-pump-thaw cycle and sealed under a prepurified and dried argon atmosphere. Solutions of the C_2 and D_3 isomers of quartet **1** in different solvent mixtures were prepared from samples of pure isomers, obtained from semipreparative HPLC chromatography,^[34] by following the next procedure. First, the target isomer was dissolved in $CHCl_3$ at low temperature and the resulting solution was evaporated quickly at reduced pressure, keeping the solution in an ice bath all the time to avoid the diastereomerization process. Second, the resulting glassy solid residue was dissolved at low temperature in the desired solvent mixture, and finally degassed with argon and frozen in a liquid N_2 bath in order to keep the solution for spectrometric measurements. Once the spectra were collected the samples were analyzed by analytical HPLC to verify that the diastereomerization had been properly quenched.

Statistical data analysis: To fit the experimental data to a physicochemical model, the Systat software (Systat, Evanston, IL, USA) was used. The statistical data obtained with the multivariate linear regression fits complied with the usual recommendations.^[35] In addition, the standard deviation of the regressions (s) and the adjusted coefficient of multiple determination (r^2) is given for each regression. The F test at 99.9% confidence level was used to indicate the significance of the independent variable coefficients.

Semiempirical calculations: All theoretical calculations described were carried out with the MOPAC 93 (Rev. 2) package.^[36] Molecular geometries were first optimized by using the AM1 hamiltonian and an UHF wavefunction. In order to accelerate the convergence of the geometry optimization, suitable symmetry constraints (C_2 and D_3 molecular symmetries) were enforced throughout the calculation, as well as the Eigenvector Following (EF) algorithm. Radical **4** was also calculated with the same methodology assuming a D_3 molecular symmetry. Initial convergence of the SCF calculation required the use of PULAY and SHIFT algorithms. GNORM test for final convergence of the optimization was set to 2×10^{-3} kJ pm⁻¹. In all cases, the energies of the electronic states and the heats of formation mentioned were estimated by using the final optimized geometries obtained under the above-mentioned conditions as input geometries for single-point CI calculations. For this purpose, keywords MECI, C.I. = (6,0), and OPEN = (3,3) were specified.

Molecular surface and volume calculations: For the determination of the molecular surfaces and volumes of the isomers of **1**, the GEPOL program was used.^[12] The geometries of both isomers used for such determinations were obtained by UHF-AM1 semiempirical minimizations. The atomic radii employed for the calculations were 170 pm for the carbon atoms, 180 pm for the chlorine, and 120 pm for the hydrogen atoms. The options assigned in the present work to the program variables "SUAVE", "SUMA", "VECTOR" and "OPESF" were "CON", "NSU", "VEN", and "SFY", respectively. The values for the "FRAD" and "NDIV" parameters used were of 0.5 and 5, respectively.^{[40],[41]}

Kinetic measurements: The isomerization rates of the C_2 isomer into the D_3 one (k) were measured in THF solutions (ca. 0.025 mM) in the temperature range of 292.5–320.5 K. Thus, a flask containing 25 mL of the solution was immersed in a thermostated bath at the desired temperature (temperature accuracy of $\pm 0.2^\circ$). After a given period of time (from few minutes to several hours), small samples were taken out, cooled in dry ice/acetone solutions to quench the isomerization process, and diluted with CH₃CN to avoid undesirable chromatographic problems, such as on-column precipitation due to sudden changes of solvent compositions. Analysis of the molar fractions of the C_2 and D_3 isomers (x_{C_2} and $x_{D_3} = 1 - x_{C_2}$) in each sample was performed by HPLC with the Equations (9) and (10), in which $\varepsilon = \varepsilon_{D_3}/\varepsilon_{C_2}$ is the ratio of molar absorptivities at $\lambda_{\max} = 383$ nm for the two isomers, and A_{C_2} and A_{D_3} are the integrated absorbances of the C_2 and D_3 isomers at the same wavelength.

$$x_{C_2} = \frac{A_{C_2} \varepsilon}{(A_{D_3} + A_{C_2} \varepsilon)} \quad (9)$$

$$x_{D_3} = \frac{A_{D_3} \varepsilon}{(A_{D_3} + A_{C_2} \varepsilon)} \quad (10)$$

The experimental ε value, determined with pure samples of both isomers at several temperatures, was 1.00 ± 0.04 and remained unchanged in the temperature range of 293–321 K. The analytical HPLC determinations were performed with the UV detector, working at 383 nm and at 293 K in order to avoid on-column interconversions. The analysis of data corresponding to the interconversion was carried out according to Equations (11) and (12),^{[37],[38]} in which \bar{k} and \bar{k} are the overall rate constants for the isomerization of the D_3 isomer to the C_2 one and that of the C_2 isomer to the D_3 , respectively.



$$x_{D_3} = \frac{K}{1 + K} - \left[\frac{K}{1 + K} - x_{D_3}^0 \right] \exp[-(\bar{k} + \bar{k})t] \quad (12)$$

$K = \bar{k}/\bar{k}$ is the apparent equilibrium constant, defined as the ratio of the isomeric molar fractions at infinite time ($K = x_{D_3}^\infty/x_{C_2}^\infty$), and $x_{D_3}^0$ is the molar fraction of the D_3 isomer at $t=0$. Least-squares treatment of the experimental data (x_{D_3} vs. t) to Equation (12) gave the \bar{k} , \bar{k} , K , and $x_{D_3}^0$

values at each temperature. By using the resulting overall rate constants, the kinetic ΔG^\ddagger , ΔH^\ddagger , and ΔS^\ddagger parameters for the isomerization processes were calculated from the Eyring equation.

Equilibration measurements: In order to obtain the apparent equilibrium constants in a given solvent and at a constant temperature, solutions of quartet **1** were subjected to continued heating for at least several half-lives and finally the isomeric ratios $x_{D_3}^\infty/x_{C_2}^\infty$ were determined by analytical HPLC chromatography. Typically, a solution of quartet **1** (3 mg) in the desired solvent (4 mL) was thermostated at each temperature and left under argon in the dark for 20 hours to reach the diastereomeric equilibrium. After that, the solution was cooled in dry ice/acetone to quench the isomerization process and then a sample (0.5 mL) was diluted with a precooled mixture of CH₃CN/THF (50:50) in a 1:3 ratio in order to avoid problems during the HPLC analysis. The D_3/C_2 isomeric ratio was determined by using an analytical HPLC column thermostated at 293 K, working with the UV detector at 240 nm, for the nonaromatic solvents, and at 340 nm for aromatic ones. Each equilibration measurement was repeated three or more times to ensure the reproducibility of the final result. As molar absorptivities of both isomers are the same regardless of the wavelength used, the equilibrium constant, $K(S_e, T_e)$, at a given temperature, T_e , in the solvent, S_e , was determined by using Equation (13), in which A_{D_3} and A_{C_2} are the integrated chromatographic peaks corresponding to the two isomers.

$$K(S_e, T_e) = A_{D_3}/A_{C_2} \quad (13)$$

Chromatographic capacity factor measurements: The analytical column was first thermostated at the temperature to be used in the experiment and then stabilized overnight, by using a 0.2 mL min⁻¹ flow rate of a THF/CH₃CN mixture with the initial working composition. Finally, the capacity factor (k') measurements were performed with a flow rate of 1 mL min⁻¹ and the UV/Vis detector working at 255 nm with about 0.6 mg mL⁻¹ of a solution of quartet **1** in THF/CH₃CN (60:40), which was previously equilibrated overnight at 300 K in the dark. The determination of capacity factors in the chromatographic experiments, in which the composition of the mobile phase was changed, was performed at a constant temperature of 303 K with mixtures of THF/CH₃CN of different volumetric compositions. Ratios of both solvents in such experiments ranged from the minimum ratio of the strong chromatographic solvent (THF) of 82% vol., necessary to avoid undesirable precipitation and on-column diastereomeric interconversions due to exceedingly long retention times, to the maximum ratio of THF of 50% vol., at which both isomers show almost the same retention times. After each k' determination, the analytical column was left to stabilize for 20 minutes at the new mobile-phase composition. It is important to emphasize that all the k' determinations at different mobile-phase compositions were completed without interruptions to avoid errors originated by experimental variations of the chromatographic conditions. All the measurements were repeated twice under similar working conditions. The determination of capacity factors of the chromatographic experiments for which the temperature was changed were performed with a fixed THF/CH₃CN composition of 40:60 within the temperature range of 283–318 K. This upper temperature limit of this range was set as the temperature at which the retention times of the different isomers are close to the dead time of the column, and the lower limit as the temperature at which an on-column interconversion of diastereomers starts to be detected. At each temperature, the column was left to stabilize for 20 minutes and the k' factor was measured two or three times in order to guarantee a good reproducibility.

Determination of the solvatochromic parameters: When not available from literature sources,^[39] the α and π^* parameters for a given solvent or a mixture of solvents were experimentally determined, with a precision of ± 0.001 , by measuring the variation of the UV/Vis spectrum of a pair of solvatochromic dyes, named A and B, following the procedure described elsewhere.^[39] In the case of the parameter α , the pair of dyes used were 4-nitroanisole (A) and 4-(2,4,6-triphenyl-pyridinio)-2,6-diphenylphenoxide (B). At a given solvent (S_e) and temperature (T_e), the parameter $\alpha(S_e, T_e)$ was determined from Equation (14), in which λ_{\max}^A and λ_{\max}^B are the maximum wavelengths of the lowest energy UV/Vis absorption bands for the dyes A and B, respectively.^[40]

$$\alpha(S_e, T_e) = [(1/\lambda_{\max}^A) + 1.873/\lambda_{\max}^B] \times 10^4 - 74.58/6.24 \quad (14)$$

Determination of solvatochromic parameter $\pi^*(S_e, T_e)$ was performed following one of the procedures described by Taft et al.^[39] by using 4-nitroanisole (A) and 1-ethyl-4-nitrobenzene (B) as solvatochromic dyes. The parameter π^* of each solvent was obtained from Equations (15)–(17), in which λ_{\max}^A and λ_{\max}^B are the wavelengths of the lowest energy UV/Vis absorption bands of the dyes A and B, respectively.

$$\pi_A^*(S_e, T_e) = [(1/\lambda_{\max}^A) \times 10^4 - 34.12] / -2.342 \quad (15)$$

$$\pi_B^*(S_e, T_e) = [(1/\lambda_{\max}^B) \times 10^4 - 34.12] / -2.342 \quad (16)$$

$$\pi^*(S_e, T_e) = [\pi_A^*(S_e, T_e) + \pi_B^*(S_e, T_e)] / 2 \quad (17)$$

Determination of the cavitation parameter: The cavity formation term, or cavitation parameter $[\Omega(S_e, T_e)]$, of a solvent S_e at a given temperature T_e was determined by following the procedure given by Hildebrand et al. [Eqs. (18)–(24)],^[41] which uses the molar enthalpies of vaporization^[42] and the density of the solvent.^[43]

$$\Omega(S_e, T_e) = c(b - aT_e)^{n+1} \quad (18)$$

$$a = d[\rho(S_e, T_e)]/dT \quad (19)$$

$$b = \rho(S_e, T_e) + d[\rho(S_e, T_e)]/dT \quad (20)$$

$$c = \frac{\exp\{2[\ln \delta_H(S_e, 298) + \frac{n+1}{2} \ln V^1(S_e, 298)]\}}{(M \times 10^{-3})^{n+1}} \quad (21)$$

$$n+1 = -2 \left[\frac{\ln \delta_H(S_e, 298) - \delta_H(S_e, T_{\text{boil}})}{\ln V^1(S_e, 298) - V^1(S_e, T_{\text{boil}})} \right] \quad (22)$$

$$\delta_H(S_e, T) = \left[\frac{\Delta H_v(S_e, T) - 1.9872 T}{V^1(S_e, T)} \right]^{1/2} \quad (23)$$

$$V^1(S_e, T) = \frac{M \times 10^{-3}}{b - aT} \quad (24)$$

In the above equations T_{boil} is the boiling temperature of the solvent, $\rho(S_e, T)$ is the density of the solvent at the temperature T , $d[\rho(S_e, T)]/dT$ is the variation of the density with the temperature at T_e , $\delta_H(S_e, T_e)$ is the Hildebrand's density at T_e , $V^1(S_e, T_e)$ is the molar volume of the solvent S_e at T_e , $\Delta H_v(S_e, T_e)$ is the molar enthalpy of vaporization at temperature T_e , and M is the molecular mass of the solvent. For a binary mixture of solvents, the cavitation parameter at the temperature T_e was calculated assuming the additivity of this magnitude by means of Equation (25), in which x_1 and x_2 are the volumetric fractions of pure solvents 1 and 2 at T_e .

$$\Omega(S_1, S_2, T_e) = x_1 \Omega(S_1, T_e) + x_2 \Omega(S_2, T_e) \quad (25)$$

Acknowledgment

This work was supported by DGES (Spain; grant: PB96-0862-C02-01), NEDO agency (Japan), and CIRIT (Catalunya; grant: 96-00106). D.R.-M. and J.S. thank to the Generalitat de Catalunya (CIRIT) for their doctoral fellowships. The authors also thank to Dr. J. Vidal-Gancedo (ICMAB, CSIC) for some ESR spectra and to Dr. D. B. Amabilino (ICMAB, CSIC) and one of the referees for their valuable comments.

[1] I. Langmuir, *Colloid. Symp. Monogr.* **195**, 3, 3.

[2] R. A. Pierotti, *Chem. Rev.* **1976**, 76, 717.

[3] L. Pauling, *Nature* **1948**, 161, 707.

[4] a) L. Connolly, *J. Appl. Crystallogr.* **1983**, 16, 548; b) B. Lee, F. M. Richards, *J. Mol. Biol.* **1971**, 55, 379; c) F. M. Richards, *Annu. Rev.*

Biophys. Bioeng. **1977**, 6, 151; d) E. Silla, I. Tuñon, J. L. Pascual-Ahuir, *J. Comp. Chem.* **1991**, 12, 1077.

[5] J. Veciana, C. Rovira, N. Ventosa, M. I. Crespo, F. Palacio, *J. Am. Chem. Soc.* **1993**, 115, 57.

[6] N. Ventosa, D. Ruiz-Molina, C. Rovira, J. Veciana in *Advances in Dendritic Macromolecules, Vol. 3* (Ed.: G. R. Newkome), JAI, Connecticut, **1996**, 27.

[7] M. J. Kamlet, R. M. Doherty, M. H. Abraham, Y. Marcus, R. W. Taft, *J. Phys. Chem.* **1988**, 92, 5244.

[8] a) D. Gust, K. Mislow, *J. Am. Chem. Soc.* **1973**, 95, 153; b) K. Mislow, *Acc. Chem. Res.* **1976**, 9, 26; c) K. P. Meurer, F. Vögtle, *Top. Curr. Chem.* **1985**, 127, 1; d) J. D. Andose, K. Mislow *J. Am. Chem. Soc.* **1974**, 96, 2168.

[9] J. Sedó, N. Ventosa, D. Ruiz-Molina, M. Mas, E. Molins, C. Rovira, J. Veciana, *Angew. Chem.* **1998**, 110, 344; *Angew. Chem. Int. Ed.* **1998**, 37, 330.

[10] M. L. Connolly, *Science* **1983**, 221, 709.

[11] J. L. Pascual-Ahuir, E. Silla, *J. Comp. Chem.* **1990**, 11, 1047.

[12] J. L. Pascual-Ahuir, E. Silla, *QCPE Program 554*, Quantum Chemistry Program Exchange Center, Bloomington (USA).

[13] a) M. Lewis, D. C. Rees, *Science* **1985**, 230, 1163; b) P. Pfeizer, U. Welz, H. Wippermann, *Chem. Phys. Lett.* **1985**, 113, 535.

[14] a) D. A. Tomalia, A. M. Naylor, W. A. Goddard, III, *Angew. Chem.* **1990**, 102, 119; *Chem. Int. Ed. Engl.* **1990**, 29, 113; b) G. R. Newkome, C. W. Moorefield, G. R. Baker, *Aldrichim. Acta* **1992**, 25, 31; c) J. M. J. Frechet, *Science* **1994**, 263, 1710; d) D. A. Tomalia, *Adv. Mater.* **1994**, 6, 529; e) G. R. Newkome, C. W. Moorefield, F. Vögtle, *Dendritic Macromolecules: Concepts, Synthesis, Perspectives*, VCH, Weinheim, **1996**.

[15] J. Veciana, C. Rovira, M. I. Crespo, O. Armet, V. M. Domingo, F. Palacio, *J. Am. Chem. Soc.* **1991**, 113, 2552.

[16] The Arrhenius plot gave $E_a = 92 \pm 2 \text{ kJ mol}^{-1}$ and $\ln A = 26 \pm 1$ for the $C_2 \rightarrow D_3$ conversion.

[17] The value of δ is equal to the number of indistinguishable positions adopted by the molecule (considered rigid) by simple rotations. For related examples of symmetry contributions to the entropy of a molecule, see ref. [24].

[18] The capacity factor k'_i of an eluant is directly related with its retention time t_r by means of $k'_i = (t_r - t_0)/t_0$, t_0 is the dead time or elution time for an unretained eluant.

[19] The separation factor α of two different eluants is defined as the ratio of the capacity factor of the most retained one, k'_2 , over that of the least retained one, k'_1 ; that is, $\alpha = k'_2/k'_1$.

[20] a) J. Chmielowiec, H. Sawatzky, *J. Chromatogr. Sci.* **1979**, 17, 245; b) W. R. Melander, B.-K. Chen, Cs. Horvath, *J. Chromatogr.* **1979**, 187, 167; c) L. R. Snyder, *J. Chromatogr.* **1979**, 179, 167; d) R. E. Boehm, D. E. Martire, D. W. Armstrong, *Anal. Chem.* **1988**, 60, 522.

[21] a) M. J. Kamlet, R. W. Taft, *J. Am. Chem. Soc.* **1976**, 98, 377, 2886; b) M. J. Kamlet, J.-L. M. Abboud, R. W. Taft, *J. Am. Chem. Soc.* **1977**, 99, 6027; M. J. Kamlet, J.-L. M. Abboud, R. W. Taft, *J. Am. Chem. Soc.* **1977**, 99, 8325; c) R. W. Taft, J.-L. M. Abboud, M. J. Kamlet, M. H. Abraham, *J. Solution Chem.* **1985**, 14, 153; d) J.-L. M. Abboud, M. J. Kamlet, R. W. Taft, *Prog. Phys. Org. Chem.* **1981**, 13, 481.

[22] P. Sadek, P. W. Carr, R. M. Doherty, M. J. Kamlet, R. W. Taft, M. H. Abraham, *Anal. Chem.* **1985**, 57, 2971.

[23] a) C. Reichardt, *Solvents and Solvent Effects in Organic Chemistry*, 2nd ed., VCH, Weinheim, New York, **1990**; b) C. Reichardt, *Chem. Rev.* **1994**, 94, 2319.

[24] G. W. Klump, *Reactivity in Organic Chemistry*, Wiley, New York, **1982**, pp. 36–50, and references therein.

[25] The α and π^* parameters were experimentally determined at 298 K and 330 K. The factors $\alpha(S_e, 330)/\alpha(S_e, 298)$ and $\pi^*(S_e, 330)/\pi^*(S_e, 298)$ were calculated for the studied solvents and used to correct the values described in the literature at 298 K. For some of the 19 studied solvents it was not possible to determine the solvatochromic parameters because of their low transparency in the absorption region of available dyes. In those cases a correction factor of 0.93 (which is the main factor found with the rest of solvents) was used to correct the π^* parameter. No corrections on the α parameter were applied, since this parameter is not affected by the temperature changes.

[26] B. Everitt, *Cluster Analysis*, Halsted, London, **1980**.

- [27] M. J. Kamlet, R. M. Doherty, M. H. Abraham, Y. Marcus, R. W. Taft, *J. Phys. Chem.* **1988**, *92*, 5244.
- [28] a) S. Lee, S.-Z. Tang, *Phys. Rev. B.* **1985**, *32*, 2761; b) S. Lee, I. M. Brown, *Phys. Rev. B* **1986**, *34*, 1442.
- [29] a) G. Kothe, E. Ohmes, J. Brickmann, H. Zimmermann, *Angew. Chem.* **1971**, *83*, 1015; *Angew. Chem. Int. Ed. Engl.* **1971**, *10*, 938; b) K. Reibish, G. Kothe, J. Brickmann, *J. Chem. Phys. Lett.* **1972**, *17*, 86; c) J. Brickmann, G. Kothe, *J. Chem. Phys.* **1973**, *59*, 2807.
- [30] I. T. Jolliffe, *Principal Component Analysis*, Springer, New York, **1986**.
- [31] X. Tomas, J. Rius, J. Obiols, A. Sol, *J. Chemometrics* **1988**, *3*, 139.
- [32] M. Fosina, R. Leardi, C. Armanino, S. Lanteri, *PARVUS: An Extendable Package of Programs for Data Exploration*, Elsevier, Amsterdam, **1988**.
- [33] M. Meloun, J. Militky, M. Forina, *Chemometrics for Analytical Chemistry, Vol. 1*, Ellis Horwood, Chichester, **1992**.
- [34] Large amounts of pure C_2 isomer are preferably obtained by recrystallization of the diastereomeric mixture of **1** in benzene.
- [35] For recommendations for reporting results of correlation analysis in chemistry by using regression analysis, see: M. Charton, S. Clementi, S. Ehrenson, O. Exner, J. Shorter, S. Wold, *Quant. Struct. Act. Relat.* **1985**, *4*, 29.
- [36] a) J. J. P. Stewart, *MOPAC 6.0, QCPE Program 455*, Quantum Chemistry Program Exchange Center, Bloomington (USA); b) J. J. P. Stewart, in *Reviews in Computational Chemistry*, (Eds.: K. B. Lipkowitz, D. B. Boyd), VCH, Weinheim, **1990**, p. 45.
- [37] The overall rate constants, \bar{k} and \bar{k} , for the studied isomerizations can be related to the rates for the reversal of the helicity of each stereogenic center, k_1 and k_2 , of the different enantiomers with D_3 and C_2 symmetries by $\bar{k} = 3k_1$ and $\bar{k} = k_2$. Both relationships have been inferred by considering the statistical factors that take into account the probabilities of each process and assuming that the diastereomerization process takes place through an uncorrelated reversal of the helicities of the three independent stereogenic elements (propellers), through an **1h** epimerization process (see Discussion), see Equation (26). In Equation (26) k_1 , k_2 , and k_3 symbolize the rate constants for the reversal of helicity of the stereoisomers, and (M,M,M) -**1** and (P,P,P) -**1** denote the two enantiomers with a D_3 symmetry and (P,M,M) -**1** and (M,P,P) -**1** describe those with a C_2 symmetry; see ref. [38].
- $$(M,M,M)\text{-}\mathbf{1} \xrightleftharpoons[k_2]{3k_1} (M,M,P)\text{-}\mathbf{1} \xrightleftharpoons[2k_3]{2k_3} (M,P,P)\text{-}\mathbf{1} \xrightleftharpoons[3k_1]{k_2} (P,P,P)\text{-}\mathbf{1} \quad (26)$$
- [38] Descriptors P and M denote *Plus* and *Minus* and describe the helicity of each $Ar_2C \cdot Ar'$ propeller-like subunit. In order to give a complete conformational description of each stereoisomer of quartet **1**, the following convention has been adopted: descriptors of the three helical subunits are ordered starting from the unique helix and following a clockwise sense.
- [39] M. J. Kamlet, J.-L. M. Abboud, R. W. Taft, *J. Am. Chem. Soc.* **1977**, *99*, 6027.
- [40] This equation was derived from that proposed by Taft et al., ref. [39]: $\alpha(S_e, T_e) = [\nu_{\max}^B - (-1.873\nu_{\max}^A + 74.58)]/6.24$, where ν_{\max}^A and ν_{\max}^B are the frequencies of UV/Vis absorption of dyes A and B, respectively, in the solvent S_e at the temperature T_e . The error in the determination of $\alpha(S_e, T_e)$ arises mainly from the precision of the wavelength measurement, which in our experiments was $\Delta\lambda = \pm 0.04$ nm.
- [41] J. H. Hildebrand, R. L. Scott, *The Solubility of Non-Electrolytes*, 3rd ed., Dover Publications, New York, **1964**, p. 424.
- [42] V. Majer, V. Svoboda, *Enthalpies of Vaporization of Organic Compounds, IUPAC Chemical Data Series no. 32*, Blackwell Scientific Publications, Oxford, **1985**.
- [43] J. A. Riddick, W. B. Bunger, *Organic Solvents*, Wiley-Interscience, New York, **1970**.

Received: November 10, 1998
Revised version: May 25, 1999 [F1432]